JJMIE

Volume 9 Number 3, June.2015
ISSN 1995-6665
Pages 195 - 207

Jordan Journal of Mechanical and Industrial Engineering

Free Vibration of an Axially Preloaded Laminated Composite Beam Carrying a Spring-Mass-Damper System with a Non-Ideal Support

Majid Ghadiri [a] *, Keramat Malekzadeh [b] , Faramarz Ashenai Ghasemi[c]

[a] *Faculty of Engineering, Department of Mechanics, Imam Khomeini International University, Qazvin, Iran.*
[b] *Department of Mechanical Engineering, Malek Ashtar University of Technology 4th Kilometer, Makhsous RD, Tehran, Iran*
[c] *Department of Mechanical Engineering, Shahid Rajaee Teacher Training University (SRTTU) Lavizan, Tehran, Iran*

Received 28 May 2014 *Accepted 28 May 2015*

Abstract

This paper investigates the effect of a non-ideal support on free vibration of an Euler-Bernoulli composite beam carrying a mass-spring-damper system under an axial force. The beam simply supported boundary conditions and it is assumed that one of its supports is non-ideal. Therefore, it has a small non-zero deflection and a small non-zero moment. The governing equations of the problem constitute a coupled system including a PDE and an ODE. To solve the problem, the Galerkin method is employed in the displacement field in conjunction with the average acceleration method in the time domain. The effect of a non-ideal support of composite beam, under axial force on natural frequencies and mode shapes of the system, is studied in details. For the validation of the performed solution and the obtained results, in a special case, the fundamental frequency was compared with those cited in the literature. The obtained results show that with increasing the perturbation parameter, the fundamental frequency decreases. This behavior is independent of the fiber directions of the beam. Also, the beams having fully-ideal supports will be buckled sooner than the beams with semi-ideal supports.

Keywords: *Beam; Free Vibration; Axial Load; Non-Ideal Support; Spring-Mass-Damper System.*

1. Introduction

Although the beams are still used as a design model for the vibration analysis of various realistic systems, most of the research studies are conducted on the vibration analysis of the beams with ideal supports and there are very few studies related to the ones having non-ideal supports.

Rayleigh [1] determined the fundamental frequency of a uniform cantilever beam carrying a tip mass. He used the static deflection curve of the beam acted upon concentrated tip load as a good estimation of fundamental mode shape estimate. Timoshenko [2] developed a series of formulae corresponding to various beam-point mass configurations. Turhan [3] studied the beams with various ideal end conditions. He presented an exact frequency equation for each case and compared the results in a broad range of relevant parameters. Matsunaga [4] analyzed the natural frequencies and buckling loads of a simply supported beam to initial axial tensile and/ or compressive forces. He applied Hamilton's principle to derive the equations of dynamic equilibrium and natural boundary conditions of a beam. He presented a one-dimensional higher order theory of thin rectangular beams to take into account the effects of both shear deformations and depth changes. He showed that with the help of his method, the natural frequencies and buckling loads of such beams could be evaluated more accurately than the previous methods. Banerjee [5] studied the free vibrations of axially loaded composite Timoshenko beams using the dynamic stiffness method. The solution technique, which he used to yield the natural frequencies, was that of the Wittrick-Williams algorithm. The effects of axial force, shear deformation and rotatory inertia on the natural frequencies were demonstrated. He showed that the shear deformation and rotatory inertia are seen to have a relatively marginal effect on the natural frequencies of this particular composite beam. However, the axial force was seen to have quite a significant effect on the fundamental natural frequency of the beam whereas it was seen to have a relatively lesser effect on other natural frequencies. He demonstrated that the natural frequency diminishes when the axial load changes from tensile to compressive, as expected. Naguleswaran [6] studied the transverse vibration of uniform Euler–Bernoulli beams linearly varying fully tensile, partly tensile or fully compressive

* Corresponding author. e-mail: ghadiri@eng.ikiu.ac.ir.

axial force distribution. He derived the general solution, expressed as the super-position of four independent power series solution functions. He showed that an increase in the values of one or both of the system parameters stiffens the system and results in an increase in the frequency parameter. He also presented that if one or both of the system parameters are negative; combinations exist for which a frequency parameter is zero. He stated that a necessary (but not sufficient) condition for the onset of buckling is when one or both system parameters are negative.

Naguleswaran [7] also studied the vibration of beams with up to three-step changes in cross-section and in which the axial force in each portion is constant but different. He showed that the Euler buckling occurs for certain combinations of the axial forces for which a frequency parameter is zero. A necessary (but not sufficient) condition for this to occur is at least one of the axial forces must be compressive.

Yesilce *et al.* [8] presented an extensive literature review of the beams carrying simply spring-mass systems and additional complexities. He also studied the effect of axial force on free vibration of Timoshenko multi-span beam with multiple attached spring-mass systems. He showed that an increase in the value of axial force causes a decrease in the frequency values; however, the amount of this decrease due to the modes is related to the number of spring-mass systems attached to the model. He also demonstrated that the frequency values show a very high decrease as a spring-mass system is attached to the bare beam; the amount of this decrease considerably increases as the number of spring-mass attachments is increased.

It is normally assumed that the ideal conditions are satisfied exactly. However, small deviations from ideal conditions in real systems occur. Pakdemirli *et al.* [9] studied the effect of non-ideal boundary conditions on the vibrations of the beams. He considered two different beam vibration problems and an axially moving string problem. He treated them using the Lindstedt-Poincare technique and the method of multiple scales. He showed that non-ideal boundary conditions may affect the frequencies as well as amplitudes of vibration. He also demonstrated that, depending on the location of non-ideal support conditions and their small variations in time, frequencies may increase or decrease. Pakdemirli *et al.* [10] also studied the non-linear vibrations of a simple-simple beam with a non-ideal support in between. He presented the approximate analytical solution of the problem using the method of multiple scales. He showed that depending on the mode shape numbers and locations, the frequencies may increase or decrease or remain unchanged. He also demonstrated that derivations from the ideal conditions lead to a drift in frequency-response curves which may be positive, negative or zero, depending on the mode number and locations.

Boyaci [11] widened the idea of non-ideal supports to a damped forced non-linear simple-simple beam vibration problem in which the nonlinearity was due to stretch effects. He combined the effects of non-linearity and non-ideal boundary conditions on the natural frequencies and mode shapes and examined them using the method of multiple scales. He stated that the stretching effect may increase the frequency while the non-ideal boundary conditions may increase or decrease them. Malekzadeh *et al.* [12] investigated the effect of non-ideal boundary conditions and initial stresses on the vibration of laminated plates on Pasternak foundation studied. The plate had simply supported boundary conditions and it was assumed that one of the edges of the plate allowed a small non-zero deflection and moment. The vibration problem was solved analytically using the Lindstedt-Poincare perturbation technique. So the frequencies and mode shapes of the plate, with a non-ideal boundary condition, was extracted by considering the Pasternak foundation and in-plane stresses. The results of the finite element simulation, using ANSYS software, were presented and compared with the analytical solution. The effect of various parameters, like stiffness of foundation, boundary conditions and inplane stresses on the vibration of the plate, was discussed. The Lindstedt-Poincare perturbation technique was used to study the effect of non-ideal boundary conditions on buckling load of laminated plates on elastic foundations by Khalili *et al.* [13]. The plate was simply supported and it was assumed that one of the edges of the plate allowed a small non-zero deflection and a small non-zero moment. The cross-ply rectangular plate rested on Pasternak foundation. The results of finite element simulations, using ANSYS FE code were presented and compared with the analytical solution. After determining the buckling load, the effect of various parameters, like stiffness of the foundation and in-plane pre-loads on the buckling load, was discussed. The proposed non-ideal boundary model was applied to the free vibration analyses of Euler-Bernoulli beam and Timoshenko beam by Jinhee [14]. The free vibration analysis of the Euler-Bernoulli beam was carried out analytically and the pseudospectral method was employed to accommodate the non-ideal boundary conditions in the analysis of the free vibration of Timoshenko beam. It was found that when the non-ideal boundary conditions are close to the ideal clamped boundary conditions, the natural frequencies are reduced noticeably as k increases. When the non-ideal boundary conditions are close to the ideal simply supported boundary conditions, however, the natural frequencies hardly change as k varies, which indicates that the proposed boundary condition model is more suitable for the non-ideal boundary condition close to the ideal clamped boundary condition. Ghadiri *et al.* [15] investigated the vibration analysis of an Euler-bernouli composite beam subjected to axial loading. The boundaries are assumed to allow small deflections and moments. So, the boundary conditions of the beam were considered as non-ideal. The governing equation of the system was solved by Lindstedt-Poincare technique. Finally, the effects of the non-ideal boundary conditions on the amplitude and frequency of vibration as well as the critical buckling load were studied.

The present paper investigates the effect of non-ideal simply supported boundary conditions under axial force on the vibration of laminated composite beams. Effect of non-ideal boundary condition on the natural frequencies and mode shapes are examined. An Euler-Bernoulli composite beam having fully-ideal (both ideal) and semi-ideal (one ideal and one non-ideal) boundary conditions under axial force is studied with the presence of an attached mass-spring-damper system. The governing equations of the beam are derived using the D'Alembert's principle. The Galerkin method is employed in the displacement field in conjunction with the average acceleration method in the time domain to solve the problem. The effect of ideal and non-ideal support of the composite beam under axial force on natural frequencies and mode shapes of the system is investigated. In order to validate the performed solution and the obtained results, in a special case, the fundamental frequency is compared with those cited in literature.

2. The Mathematical Model and Formulation

A laminated composite beam is considered, as shown in Figure 1. The governing equations of the uniform beam with an attached spring-mass system could be derived with the help of equilibrium of the dynamic forces by the D'Alembert's principle as follows [16]:

$$D\frac{\partial^4 w}{\partial x^4}+\rho A\frac{\partial^2 w}{\partial t^2}-P\frac{\partial^2 w}{\partial x^2}=f(x) \tag{1}$$

Considering Eq. (1) and Figure 1, *f(x)* could be defined as follow as:

$$f(x)=\left[F+mg\right]\delta(x-x_o) \tag{2}$$

Therefore, Eq. (1) could be written as:

$$D\frac{\partial^4 w}{\partial x^4}+\rho A\frac{\partial^2 w}{\partial t^2}-P\frac{\partial^2 w}{\partial x^2}= \tag{3}$$

$$[mg-m\,\ddot{y}(t)]\,\delta(x-x_0) \qquad t>0$$

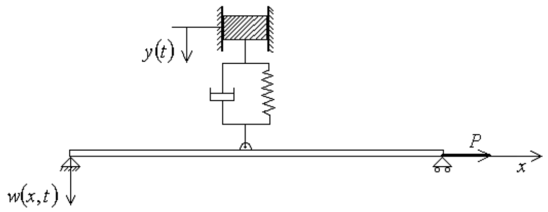

Figure 1. A schematic view of an Euler-Bernoulli laminated beam

where D is the reduced bending stiffness and $w(x,t)$ is the transverse displacement of the beam. $y(t)$ is the displacement of the attached mass relative to base level, ρ, A, L and m are density, cross section, length and amount of the attached mass to the beam, respectively. Also $\delta(x-x_0)$ is the Dirac delta function.

The reduced bending stiffness is as follows [17]:

$$D=D_{11}-\frac{\left(B_{11}\right)^2}{A_{11}} \tag{4}$$

where:

$$A_{11}=b\sum_{k=1}^{n}\left(\overline{Q}_{11}^{k}\right)_k\left(z_k-z_{k-1}\right), \tag{5}$$

$$B_{11}=\left(\frac{b}{2}\right)\sum_{k=1}^{n}\left(\overline{Q}_{11}^{k}\right)_k\left(z_k^2-z_{k-1}^2\right), \tag{6}$$

$$D_{11}=\left(\frac{b}{3}\right)\sum_{k=1}^{n}\left(\overline{Q}_{11}^{k}\right)_k\left(z_k^3-z_{k-1}^3\right) \tag{7}$$

$$\overline{Q}_{11}^{k}=Q_{11}^{k}\cos^4\phi+Q_{22}^{k}\sin^4\phi+2\left(Q_{11}^{k}+2Q_{66}^{k}\right)\cos^2\phi\sin^2\phi \tag{8}$$

$$Q_{11}=\frac{E_{11}}{1-\upsilon_{12}\upsilon_{21}} \tag{9}$$

$$Q_{22}=\frac{E_{22}}{1-\upsilon_{12}\upsilon_{21}} \tag{10}$$

$$Q_{66}=G_{12} \tag{11}$$

$$\upsilon_{21}=\frac{\upsilon_{12}E_{22}}{E_{11}} \tag{12}$$

where A_{11} is the extensional stiffness, B_{11} is the coupling stiffness, D_{11} is the bending stiffness, $\overline{Q}_{11}^{k}$ is the coefficient of reduced stiffness of the lamina, b is the width, H is the height, n_i is the number of plies, E_{11} and E_{22} are the longitudinal and transverse Young's moduli, respectively, G_{12} is the in-plane shear modulus, υ_{12} and υ_{21} are the longitudinal and transverse Poisson's ratio, respectively, ϕ is the angle of the k^{th} lamina orientation and z_k and z_{k-1} are the locations of the k^{th} lamina with respect to the midplane of beam (Figure 2) [17,18]:

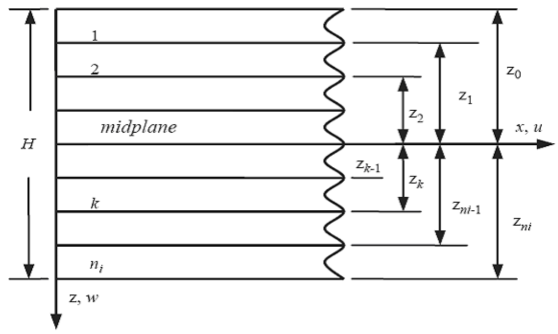

Figure 2. A schematic view of the stacking sequence of the laminated beam.

From Figure 1, the governing equation of the attached mass could be written as follows:

$$k\,y+c\dot{y}+m\ddot{y}=k\,w+c\,\dot{w} \tag{13}$$

For writing the governing equations of the problem, i.e., Eqs. (3) and (13), in their dimensionless forms, the relations between the dimensional and dimensionless (denoted by "‾") quantities are defined:

$$\bar{x}=\frac{x}{L}\ ;\quad \bar{t}=\Omega\,t\ ;\quad \Omega=\frac{1}{L^2}\sqrt{\frac{D}{\rho A}}\ ;\quad \bar{w}=\frac{\Omega^2\,w}{g}\ ;$$

$$\bar{y}=\frac{\Omega^2\,y}{g}\ ;\quad \bar{k}=\frac{k\,L^3}{D}\ ;\quad \bar{m}=\frac{m}{\rho L}\ ;\quad \bar{\delta}(0)=L\,\delta(0)\ ; \tag{14}$$

$$\bar{c}=\frac{c\,L^3}{D}\Omega\ ;\quad \bar{p}=\frac{p}{\rho\,\Omega^2\,L^2}\ ;$$

Substituting the above dimensionless quantities into Eqs. (3) and (13), the dimensionless defining equations of the behavior of the beam and its attached mass could be written as:

$$\frac{\partial^4 \bar{w}}{\partial \bar{x}^4}+\frac{\partial^2 \bar{w}}{\partial \bar{t}^2}-\bar{p}\frac{\partial^2 \bar{w}}{\partial \bar{x}^2}=\bar{m}\left(1-\ddot{\bar{y}}\right)\bar{\delta}\left(\bar{x}-\bar{x}_o\right); \quad \bar{t}>0 \tag{15}$$

$$\bar{k}\,\bar{y}+\bar{c}\,\dot{\bar{y}}+\bar{m}\,\ddot{\bar{y}}=\bar{k}\,\bar{w}+\bar{c}\,\dot{\bar{w}}; \quad \bar{x}=\bar{x}_o, \quad \bar{t}>0 \tag{16}$$

Hereinafter, we simplify the above equations by removing the "‾" symbol.

In general form, the dimensionless governing equations of an Euler-Bernoulli composite beam with an attached spring-mass-damper system could be written as:

$$\frac{\partial^4 w}{\partial x^4}+\frac{\partial^2 w}{\partial t^2}-p\frac{\partial^2 w}{\partial x^2}=m\left(1-\ddot{y}\right)\delta\left(x-x_o\right); \quad t>0 \tag{17}$$

$$k\,y+c\dot{y}+m\ddot{y}=kw+c\dot{w}; \quad x=x_o, \quad t>0 \tag{18}$$

The boundary condition of the problem is as:

$$w(0,t)=0; \qquad \frac{\partial^2 w(0,t)}{\partial^2 x}=0;$$
$$w(1,t)=\varepsilon a(t); \qquad \frac{\partial^2 w(1,t)}{\partial^2 x}=\varepsilon b(t) \tag{19}$$

ε is small perturbation parameter denoting that the variations in deflections and moments are not zero but small at the end of the beam (here, at the right end of the beam). The symbol "1" in (1,*t*) shows this non-ideal condition at the right end of the beam.

Having the same time variations in the boundaries, the following equations must be satisfied:

$$w(1,t)=\varepsilon a; \qquad \frac{\partial^2 w(1,t)}{\partial^2 x}=\varepsilon b \tag{20}$$

where a and b are constant amplitudes and are: $a=b=1$ [9].

3. The Solution Method

To solve the coupled Eqs. (17) and (18), the Galerkin's method in coordinate domain and the method of average acceleration to time discretizing are employed. The test function should be predicted in a proper way to satisfy the boundary conditions of the problem. It must be noted that in ideal support condition ($\varepsilon = 0$), the test function must satisfy the boundary conditions of the problem too. Therefore,

$$\phi_n(x)=\sin(n\pi x)+\varepsilon\left(cx^3+dx^2\right); \quad 0<x<1 \tag{21}$$

where c and d could be determined with the help of boundary conditions. Therefore, the test function is:

$$\phi_n(x)=sin(n\pi\, x)+\varepsilon\left(\frac{11}{6}x^3-\frac{5}{6}x^4\right); \quad 0<x<1 \tag{22}$$

It is seen that for $\varepsilon = 0$ (ideal boundary conditions), $\phi_n(x)$ could satisfy the boundary conditions of the problem too.

Finding the test function, $w(x,t)$ is considered as follows:

$$w(x,t)=\sum_{n=1}^{\infty}\phi_n(x)\,\alpha_n(t) \tag{23}$$

where $\alpha_n(t)$ is the time dependent functions.

Substituting the above equations into Eqs. (17) and (18):

$$\sum_{n=1}^{\infty}\phi_n''''(x)\,\alpha_n(t)+\sum_{n=1}^{\infty}\phi_n(x)\,\ddot{\alpha}_n(t)-p\sum_{n=1}^{\infty}\phi_n''(x)\,\alpha_n(t)=m\left(1-\ddot{y}\right)\delta\left(x-x_o\right); \quad t>0 \tag{24}$$

$$k\,y+c\dot{y}+m\ddot{y}=k\sum_{n=1}^{\infty}\phi_n(x)\,\alpha_n(t)+c\sum_{n=1}^{\infty}\phi_n(x)\,\dot{\alpha}_n(t); \quad x=x_o, \quad t>0 \tag{25}$$

Considering the Galerkin's method, the weight function could be chosen as:

$$\phi_m(x)=sin(m\pi\, x)+\varepsilon\left(\frac{11}{6}x^3-\frac{5}{6}x^4\right); \quad 0<x<1 \tag{26}$$

Multiplying the above equation in Eq. (24) and integrating on $0<x<1$:

$$\int_0^1\phi_m(x)\sum_{n=1}^{\infty}\phi_n''''(x)\,\alpha_n(t)dx+\int_0^1\phi_m(x)\sum_{n=1}^{\infty}\phi_n(x)\,\ddot{\alpha}_n(t)dx-p\int_0^1\phi_m(x)\sum_{n=1}^{\infty}\phi_n''(x)\,\alpha_n(t)dx=\int_0^1\phi_m(x)m\left(1-\ddot{y}\right)\delta\left(x-x_o\right)dx; \quad t>0 \tag{27}$$

The above equations could be simplified with the help of orthogonality condition.

The method of average acceleration is employed for discretizing the time. This method is mostly used in finite element analysis of time discretized dynamic equations. In this method, estimations of finite differences for displacement and velocity could be found using of Taylor's series as follows [19]:

$$\dot{w}^{t+\Delta t}=\dot{w}^{t}+\ddot{w}^{t}\Delta t \tag{28}$$

$$w^{t+\Delta t}=w^{t}+\dot{w}^{t}\Delta t+\ddot{w}^{t}\frac{\Delta t}{2} \tag{29}$$

where w is a time dependent variable, Δt is the time step size and the superscripts show the time in which the proposed expression must be calculated.

In average acceleration method, the additional assumption is:

$$\ddot{w}^{t} \Rightarrow \frac{\ddot{w}^{t+\Delta t}+\ddot{w}^{t}}{2} \tag{30}$$

where $\Rightarrow$ denotes substituting. Therefore, substituting Eq. (30) in Eqs. (28) and (29):

$$\dot{w}^{t+\Delta t}=\dot{w}^{t}+a_1\ddot{w}^{t}+a_2\ddot{w}^{t+\Delta t}=c1w\left(\dot{w}^{t},\ddot{w}^{t}\right)+a_2\ddot{w}^{t+\Delta t} \tag{31}$$

$$w^{t+\Delta t}=w^{t}+a_3\dot{w}^{t}+a_4\ddot{w}^{t}+a_5\ddot{w}^{t+\Delta t}=c2w\left(w,\dot{w}^{t},\ddot{w}^{t}\right)+a_5\ddot{w}^{t+\Delta t} \tag{32}$$

where a_i is equal to:

$$a_1=\frac{\Delta t}{2}\ ;\ a_2=\frac{\Delta t}{2}\ ;\ a_3=\Delta t\ ;\ a_4=\frac{\Delta t^2}{4}\ ;\ a_5=\frac{\Delta t^2}{4} \tag{33}$$

and $c1w$ and $c2w$ show the expressions which are as follows:

$$c1w\left(\dot{w}^{t},\ddot{w}^{t}\right)=\dot{w}^{t}+a_1\ddot{w}^{t} \tag{34}$$

$$c2w\left(w^{t},\dot{w}^{t},\ddot{w}^{t}\right)=w^{t}+a_3\dot{w}^{t}+a_4\ddot{w}^{t} \tag{35}$$

With this method, the linear differential equations would be reduced to a system of linear algebraic equations including acceleration in time $t+\Delta t$, displacement, velocity and acceleration in time t [19].

Noticing Eqs. (31) and (32), variables of the system of equations could be defined as:

$$\dot{\alpha}_n^{t+\Delta t}=\dot{\alpha}_n^{t}+a_1\ddot{\alpha}_n^{t}+a_2\ddot{\alpha}_n^{t+\Delta t}=c1\alpha\left(\dot{\alpha}_n^{t},\ddot{\alpha}_n^{t}\right)+a_2\ddot{\alpha}_n^{t+\Delta t} \tag{36}$$

$$\alpha_n^{t+\Delta t}=\alpha_n^{t}+a_3\dot{\alpha}_n^{t}+a_4\ddot{\alpha}_n^{t}+a_5\ddot{\alpha}_n^{t+\Delta t}=c2\alpha\left(\alpha_n,\dot{\alpha}_n^{t},\ddot{\alpha}_n^{t}\right)+a_5\ddot{\alpha}_n^{t+\Delta t} \tag{37}$$

Substituting the above equations in the motion equations of the system, linear partial differential equations would be changed to linear algebraic equations. The above equations could be defined as time discretized equations that $\alpha(t)$ is its unknown parameter. In order to avoid lengthy explanations, the motion equations are not shown after the above-mentioned substitution. Solving the resulted system of algebraic equations simultaneously, having the value of variables in time t, the corresponding values could be easily determined in time $t+\Delta t$.

4. Calculation of Fundamental Natural Frequency

The equation of fundamental natural frequency of a simply supported beam with one non ideal boundary condition and carrying a spring-mass system is derived using Rayleigh's method as follow as [16]:

$$T_{\max}=V_{\max} \tag{38}$$

where V_{max} is maximum potential energy and T_{max} is maximum kinematics energy of the total system. Assuming identical phase for beam and the attached mass oscillations, the maximum kinetic energy can be calculated as follows:

$$T_{\max}=T_{beam}+T_{mass}$$

$$T_{\max}=\frac{1}{2}\rho A\omega^2\int_0^l W(x)^2\,dx+\frac{1}{2}m\omega^2Y^2 \tag{39}$$

which ω is a fundamental natural frequency of the system, $W(x)$ and Y are transverse deflections of beam and the attached mass to it, respectively. Using Eq. (26), the first mode shape can be considered as:

$$W(x)=\phi_1(x)=\sin(\pi\,x)+\varepsilon\left(\frac{11}{6}x^3-\frac{5}{6}x^4\right)\ ; \tag{40}$$

The beam and the mass attached to it are supposed to oscillate with the same phase and fundamental frequency.

The maximum potential energy can be calculated as follows:

$$V_{\max}=V_{beam}+V_{mass} \tag{41}$$

and

$$V_{\max}=\frac{1}{2}k(Y-W(x_0))^2+D\int_0^l W(x)''\,dx \tag{42}$$

where,

$$mg=k(Y-W(x_0)) \tag{43}$$

Therefore, the fundamental natural frequency of a simply supported beam with one non ideal boundary condition and carrying spring-mass system is given as follows:

5. Model Verification

The fundamental frequency of the composite beam with ideal supports, which is derived with the help of Eq. (44), is compared to the calculated one by [3] for a concentrated mass without a spring. To model the present spring-mass system with a system consisting of one concentrated mass only, the spring constant k is tended to infinity. The first, second and third rows of Table 1 show that a good verification is reached for the case of ideal supports. Table 1 also demonstrates that with the increase of ε, the fundamental natural frequency decreases.

$$\omega_1^2=\frac{\frac{(mg)^2}{k}+D\int_0^1\left[-\pi^2\sin(\pi\,x)+\varepsilon(-10\,x^2+11\,x)\right]^2dx}{m\left[\frac{mg}{k}+\sin(\pi\,x_0)+\varepsilon\left(\frac{11}{6}x_0^3-\frac{5}{6}x_0^4\right)\right]^2+\rho A\int_0^1\left[\sin(\pi\,x)+\varepsilon\left(\frac{11}{6}\,x^3-\frac{5}{6}\,x^4\right)\right]^2dx} \tag{44}$$

Table1. Verification of the present method with [3], in comparison with first fundamental frequency of beam

Distance of the concentrated mass from the left side of beam support	$x_0 = 0.1$	$x_0 = 0.2$	$x_0 = 0.3$	$x_0 = 0.4$	$x_0 = 0.5$
Ideal supports ($\varepsilon = 0.0$) [3]	120.628	80.869	64.204	56.978	54.901
Ideal supports ($\varepsilon = 0.0$) [Present method (Eq. (44))]	122.726	82.384	65.335	57.722	55.218
Non-Ideal support ($\varepsilon = 0.1$) [Present method (Eq. (44))]	118.841	82.039	63.707	55.199	52.418
Non-Ideal Support ($\varepsilon = 0.2$) [Present Method (Eq. (44))]	113.083	80.869	64.204	56.978	49.770

6. Numerical Analysis and Discussions

All numerical analyses of the present paper are obtained based on the following data [17]:

$m = 2\,kg$; $L = 1\,m$; $A = 2.4 \times 10^{-4}\, m^2$;

$\rho = 1480 kg / m^3$; $x_o = 0.5\,m$;

$E_{11} = 134 \times 10^9\ N/m^2$;

$E_{22} = 10.3 \times 10^9\ N/m^2$;

$G_{12} = 5 \times 10^9\ N/m^2$; $\upsilon_{12} = 0.33$;

$b = 30 \times 10^{-3}\,m$; $\Delta t = 0.005$;

$H = 8 \times 10^{-3}\,m$; $k = 5 \times 10^3\ N/m$;

$y(t = 0) = 0.144$;

In all of the presented results, in form of time dependent curves, the oscillation amplitude of the beam is determined and drawn at the point: $x = x_0$.

It is worth mentioning that for the sake of the facility of the calculations, Matlab software is used to get the results.

7. Effect of Non-Ideal Support

Figure 3 illustrates a comparison of the first four mode shapes of the composite beam with different perturbation parameters. The layer sequence of the laminated composite beam is $[90\ 60\ 30\ 0]_s$. It is observed that the mode shapes of the beam with two ideal supports are different from the mode shapes of the beam with non-ideal support. It means that as one of the supports is non ideal ($\varepsilon = 0.1$), the amplitude of mode shape is higher.

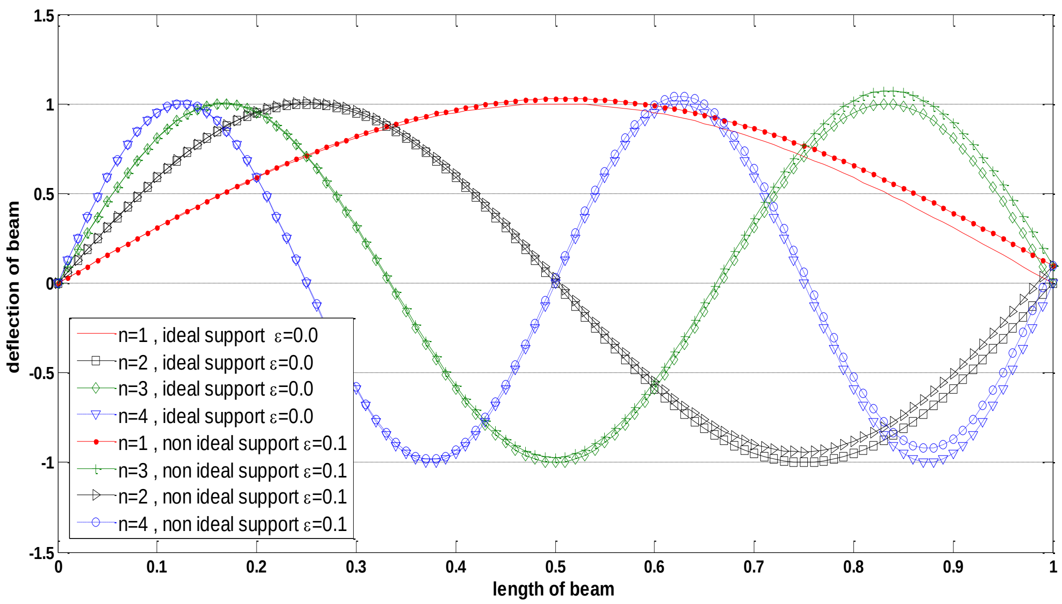

Figure 3. Comparison of mode shapes of the beam in the cases of two ideal supports and one non-ideal and one ideal support

The oscillation amplitude of the middle point of the beam and its attached mass for different perturbation parameter are shown in Figures 4 and 5, respectively. The beam is considered as a composite laminate having 8 plies which its layer sequence is: $[90\ 60\ 30\ 0]_s$. The mass oscillation is begun from point $y\ (t = 0) = 0.144$ that is given to the mass as an initial condition.

Figure 4 shows that the increase in ε causes an increase in the oscillation amplitude and the phase difference between the oscillations amplitudes.

Figure 5 shows that with increasing the perturbation parameter, the oscillations amplitude of the attached mass to the beam decreases.

The oscillations amplitude of the middle point of the beam and its attached mass with two ideal supports are shown in Figures 6 and 7, respectively. The effect of fiber directions on the oscillation of the beam and its attached mass could be seen in these figures, respectively. It is seen that in some fiber directions, the oscillation amplitude of the middle point of beam decreases. For instance, the oscillation amplitude of the middle point of the beam decreases in unsymmetrical fiber directions. Whereas the effect of the fiber directions on the oscillation amplitude of the attached mass is only a phase difference.

The effect of the fiber directions on the oscillation amplitude of the beam and its attached mass with a non-ideal support ($\varepsilon = 0.1$) are shown in Figures 8 and 9, respectively.

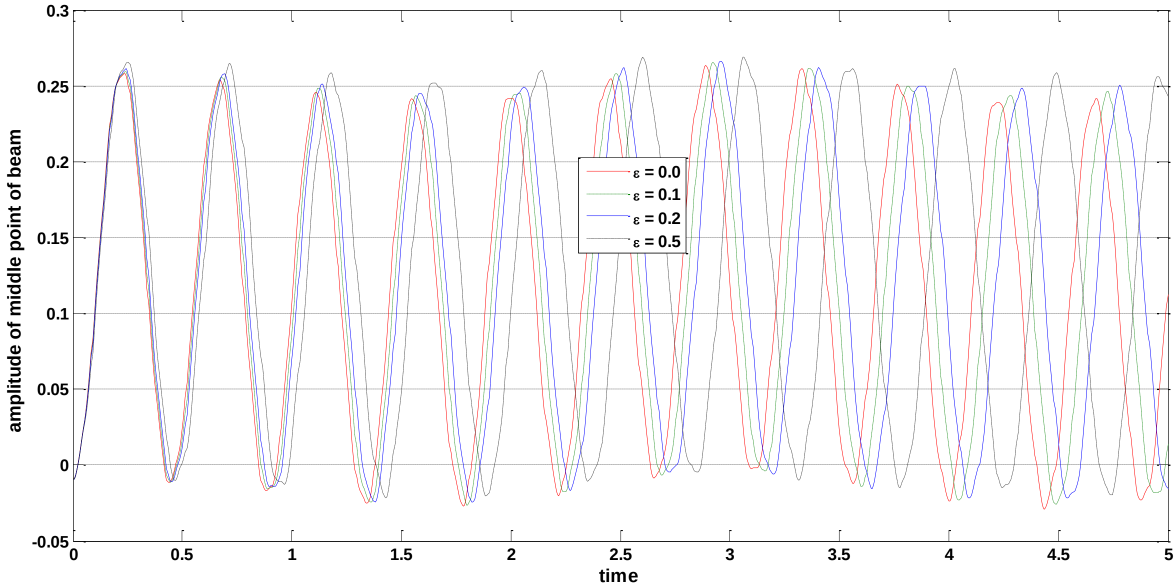

Figure 4. Comparison of vibrations of middle point of beam for different perturbation parameter

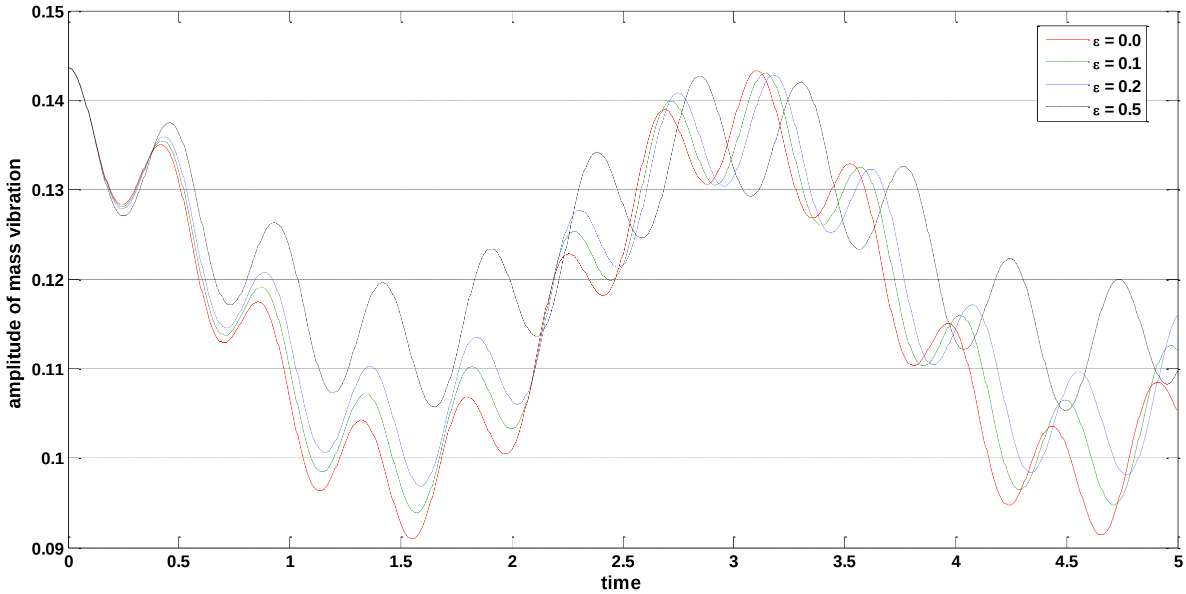

Figure 5. Comparison of vibrations of the attached mass to beam for different perturbation parameter.

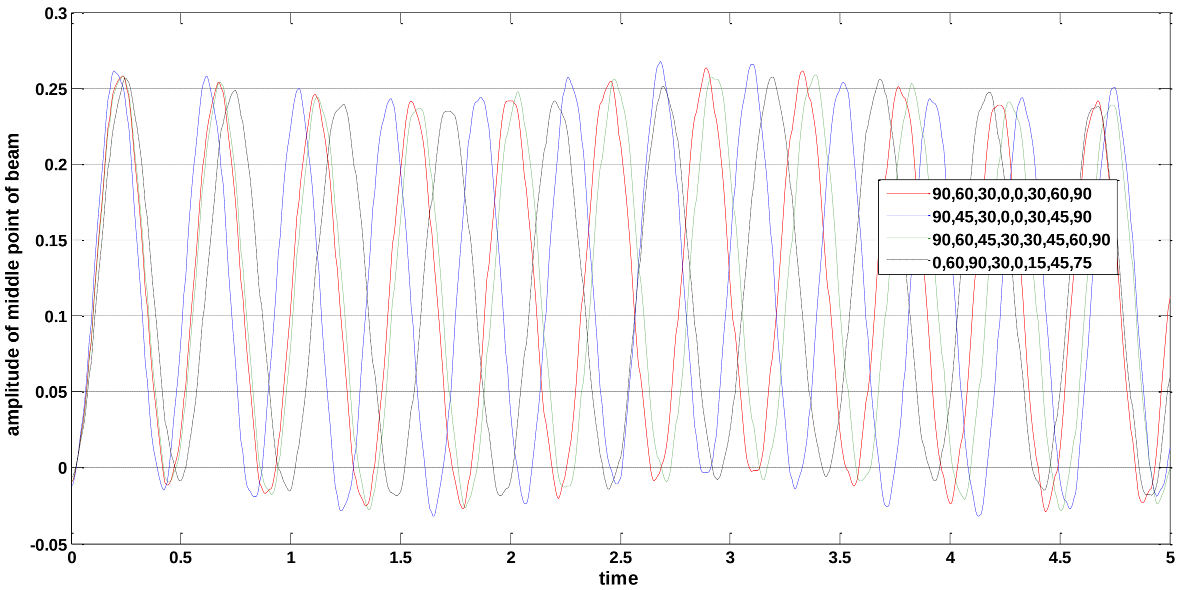

Figure 6. Comparison of vibration of the middle point of beam with two ideal supports for different fiber directions

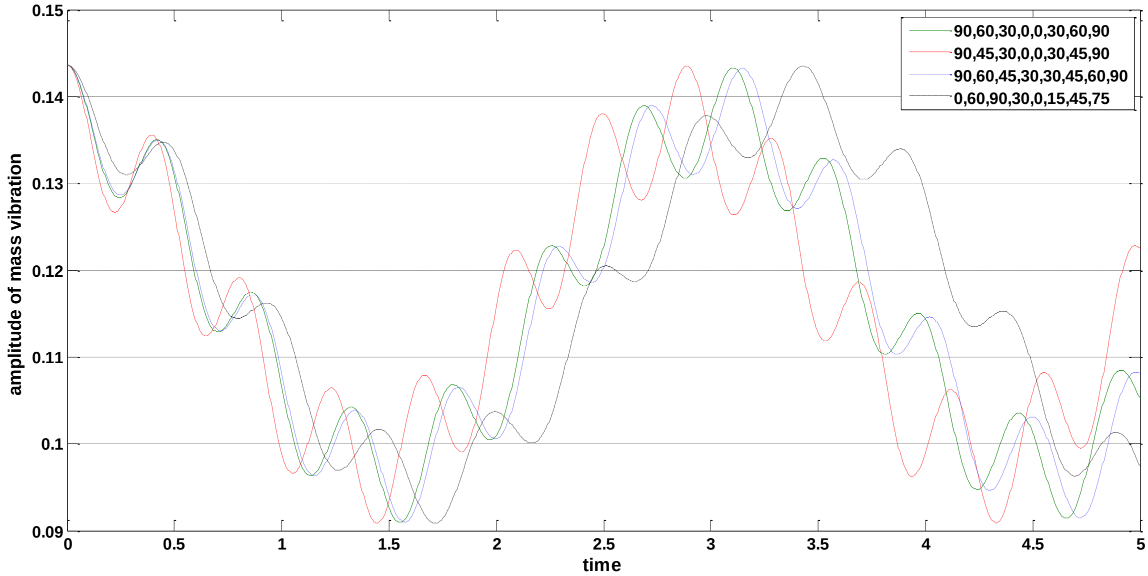

Figure 7. Comparison of vibration of the attached mass to beam with two ideal supports for different fiber directions

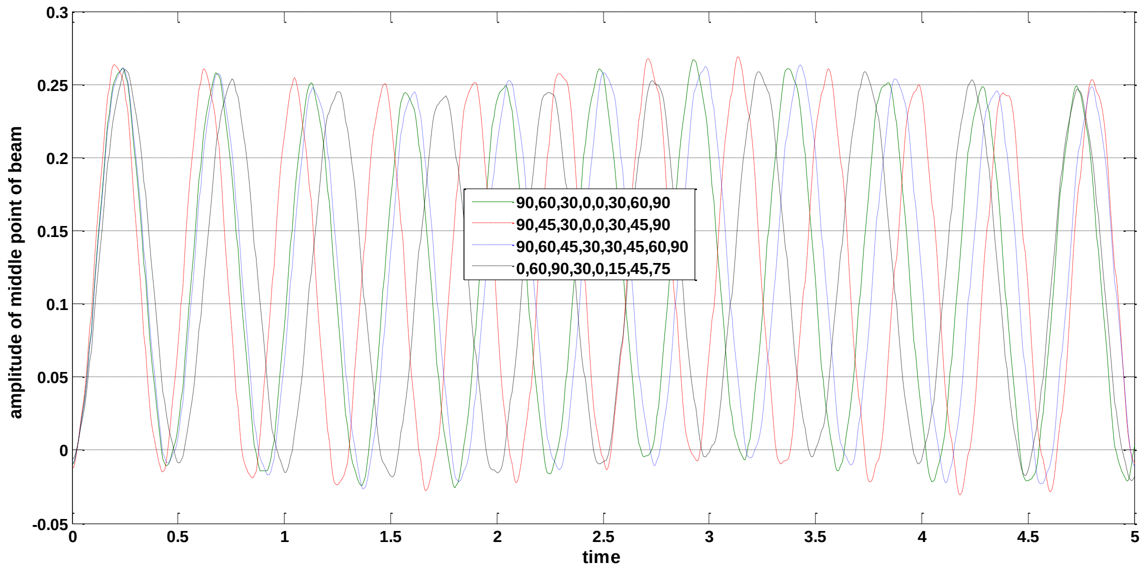

Figure 8. Comparison of vibration of the middle point of beam with one non-ideal support ($\varepsilon = 0.1$) for different fiber directions

Table 2. The effect of fiber directions of beam on its bending stiffness (*D*).

Fiber Directions	Bending Stiffness of the Beam (D)
$[90,60,30,0]_s$	100.03
$[90,45,30,0]_s$	76.47
$[90,60,45,30]_s$	105.64
[0,60,90,30,0,15,45,75]	153.56

Considering Table 2 and figures 8 and 9, it is visible that the bending stiffness of the beam with the unsymmetrical fiber directions is more than the symmetric ones. This leads to a reduction in the oscillation amplitude of the beam. Figures 8 and 9 also show that the effect of the different bending stiffness on the oscillation amplitude of the attached mass is only a phase difference.

Figure 10 shows the behavior of the fundamental frequency of the whole system (including the beam and its attached mass) with respect to the perturbation parameter (ε) for the different fiber directions.

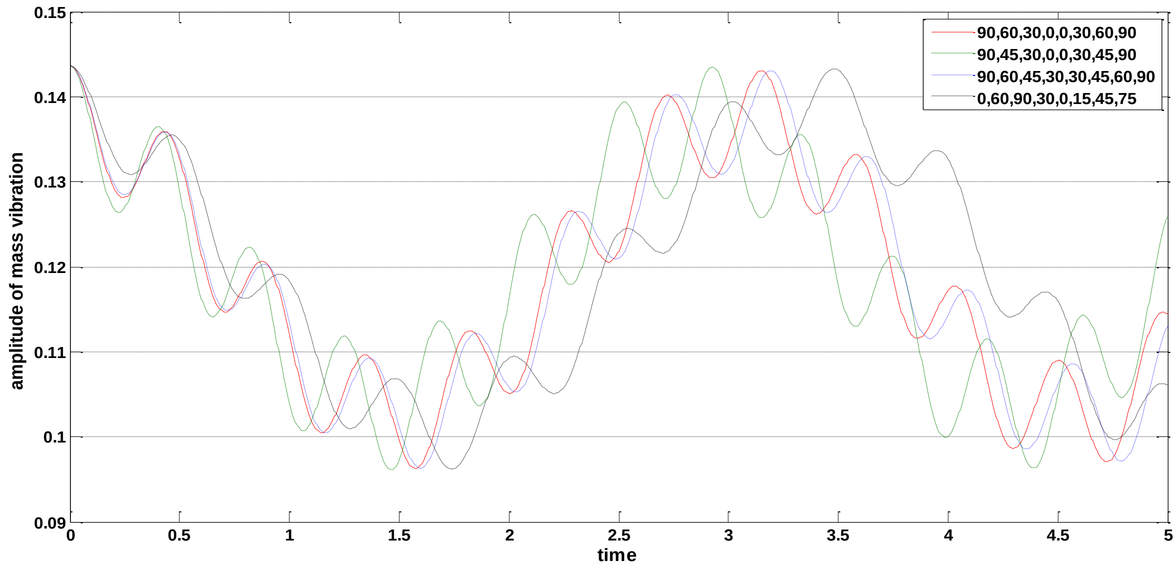

Figure 9. Comparison of vibration of the attached mass to beam with one non-ideal support ($\varepsilon = 0.1$) for different fiber directions

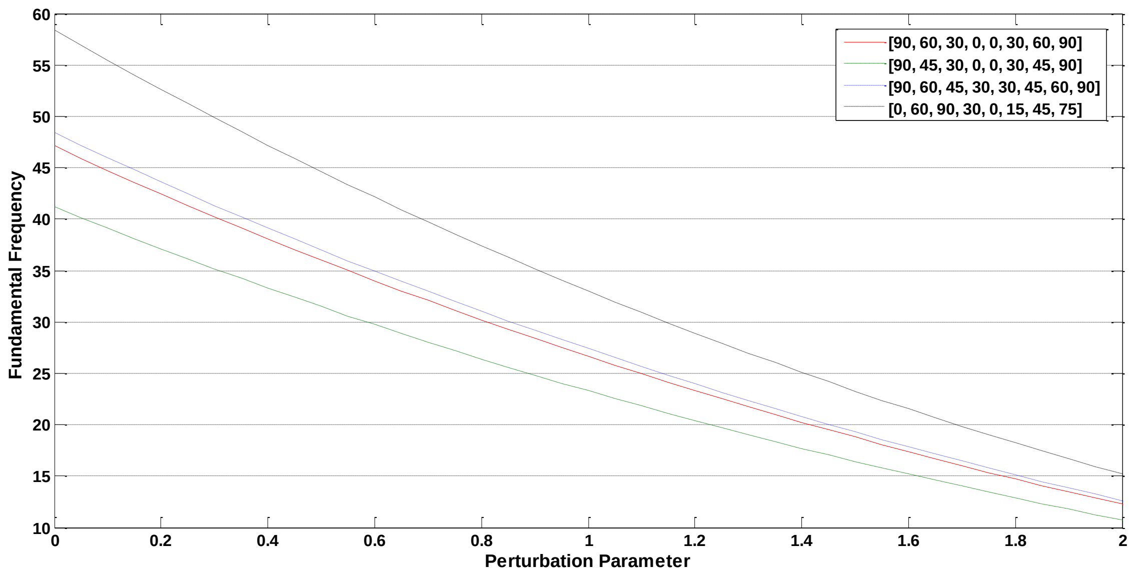

Figure 10. Comparison of vibration of the whole system with respect to perturbation parameter (ε) for different fiber directions

It is seen that for the unsymmetrical fiber directions, the fundamental is the most frequency. The more perturbation parameter is, the less fundamental frequency (no matter whether the fiber directions are symmetric or unsymmetrical).

The effect of the tensile and the compressive force on dimensionless oscillation amplitude of a laminated beam with constant fiber directions $[90\ 60\ 30\ 0]_s$ for fully-ideal and semi-ideal (having one support with ε= 0.1) supports is shown in Figures 11 and 12, respectively. The more tensile axial force, the less oscillation amplitude of the beam. Figures 11 and 12 show that increasing the compressive axial force (smaller than the axial force of the first buckling mode of the beam), increases the average of dimensionless oscillation amplitude of the middle point of beam. Because the compressive axial force decreases the bending stiffness of the beam, therefore, the average of dimensionless oscillation amplitude of the beam increases.

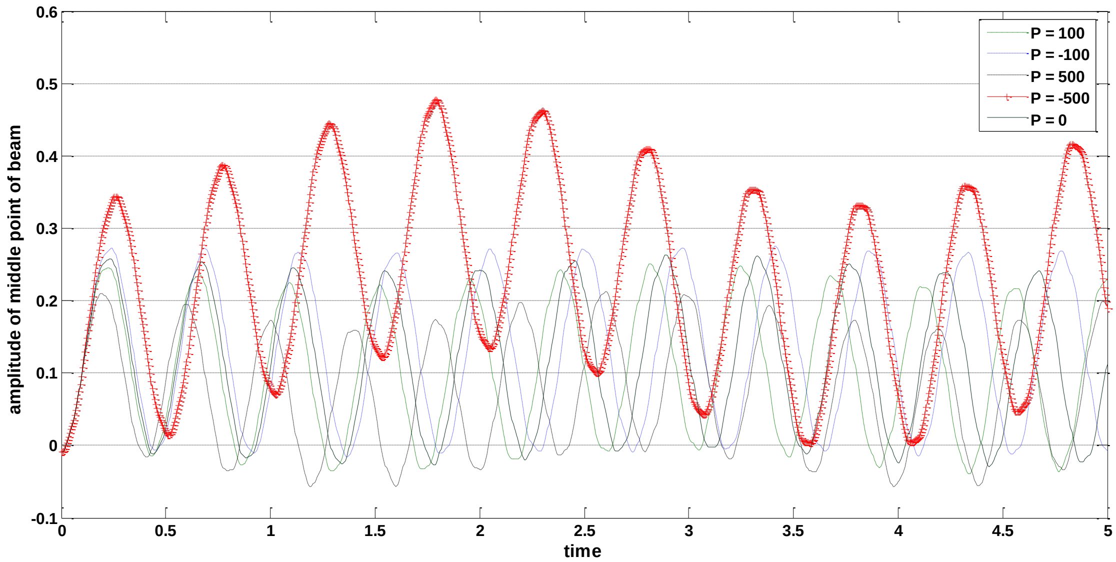

Figure 11. Comparison of vibration of the mid-point of the beam with fully-ideal supports for different axial forces

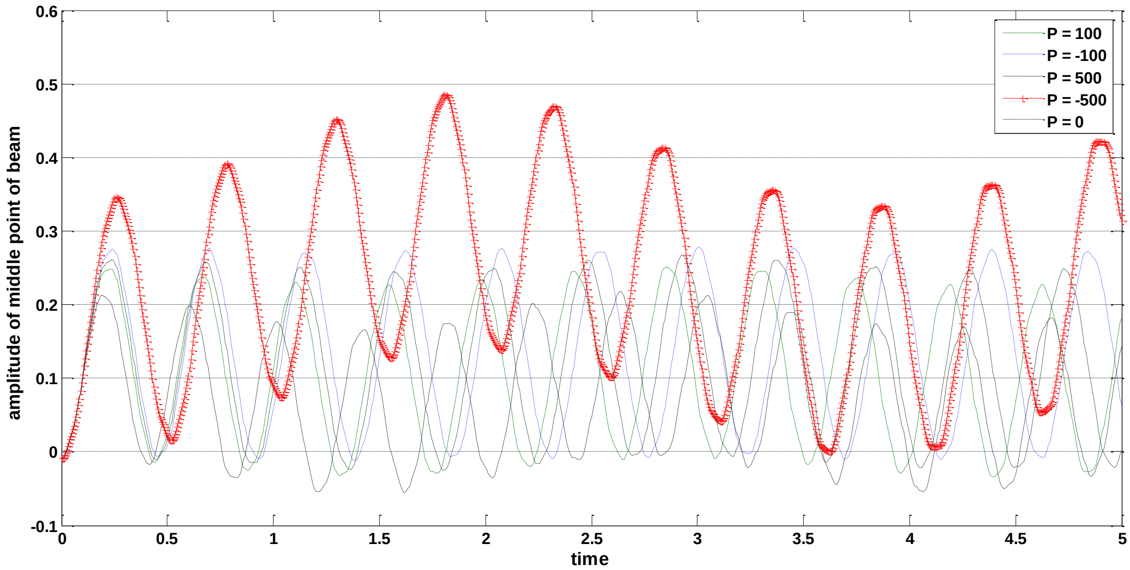

Figure 12. Comparison of vibration of the mid-point of the beam with semi-ideal supports (ε= 0.1) for different axial forces

The effect of the tensile and the compressive axial forces on dimensionless oscillation amplitude of the attached mass to the composite beam with constant fiber directions $[90\ 60\ 30\ 0]_s$ for fully-ideal and semi-ideal (ε = 0.1) supports is shown in Figures 13 and 14, respectively. No matter whether the axial force is tensile or compressive, for the case of semi ideal supports (ε = 0.1), it leads to an increase in the oscillation motion of the attached mass to the beam. When the axial force is tensile, the oscillation amplitude tends to the equilibrium point (i.e., the point that amplitude is equal to zero). The mass begins its oscillation from the point $y(t = 0) = 0.144$ that is given initial condition. Also, the compressive axial force increases the oscillation amplitude of the attached mass. This is because of the variation of the bending stiffness of the beam due to axial force.

The effect of the non-ideal supports in the reduction of the buckling probability of a laminated composite beam with the constant symmetric fiber directions [90 60 30 0]s under a compressive axial force (P = -2000 N), near the first mode of the buckling load is shown in Figure 15. It is seen that having a non-ideal support postpones the buckling of a beam under compressive forces near the first mode of the buckling load. Therefore, a beam with fully-ideal supports will be buckled sooner than with semi-ideal ones at the same loading condition.

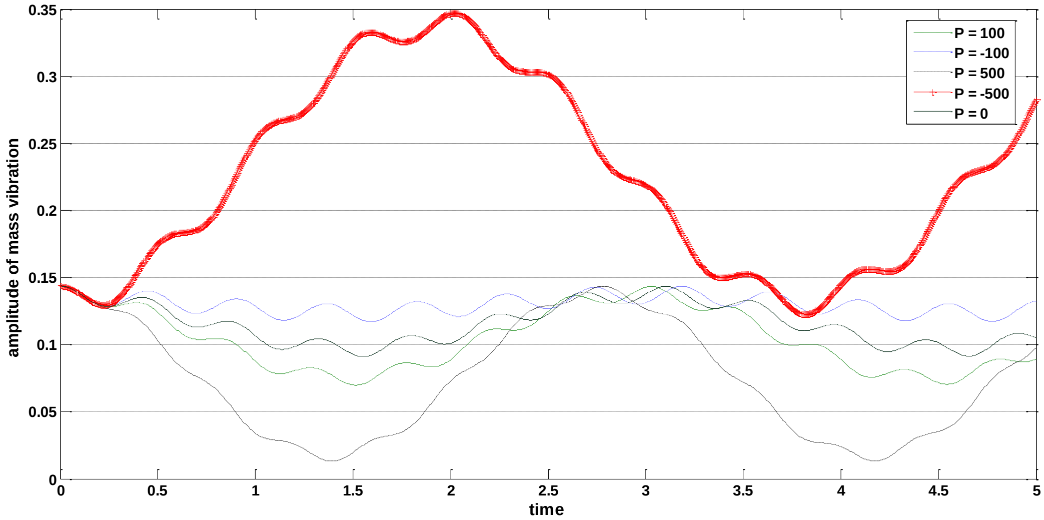

Figure 13. Comparison of vibration of the attached mass to beam with fully-ideal supports for different axial forces

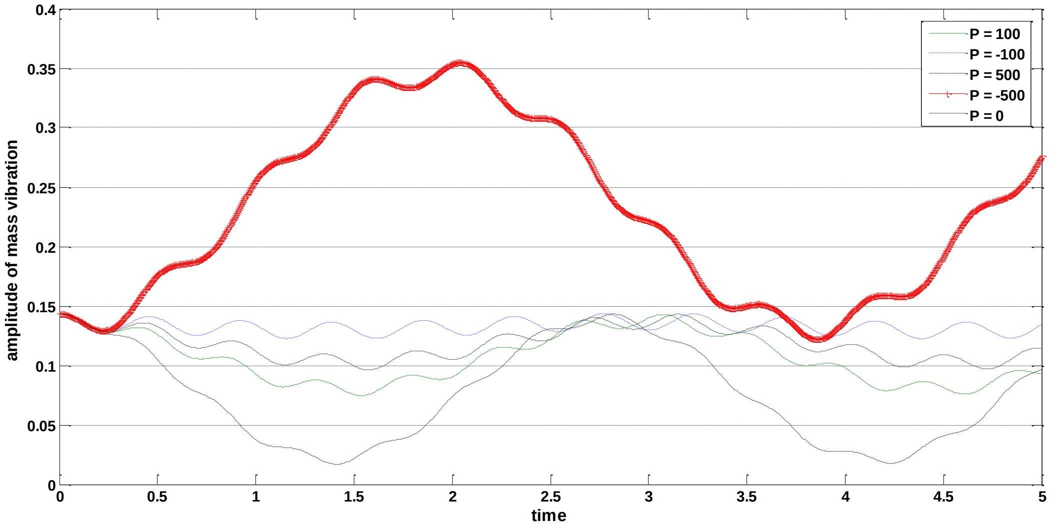

Figure 14. Comparison of vibration of the attached mass to beam with semi-ideal (ε = 0.1) supports for different axial forces

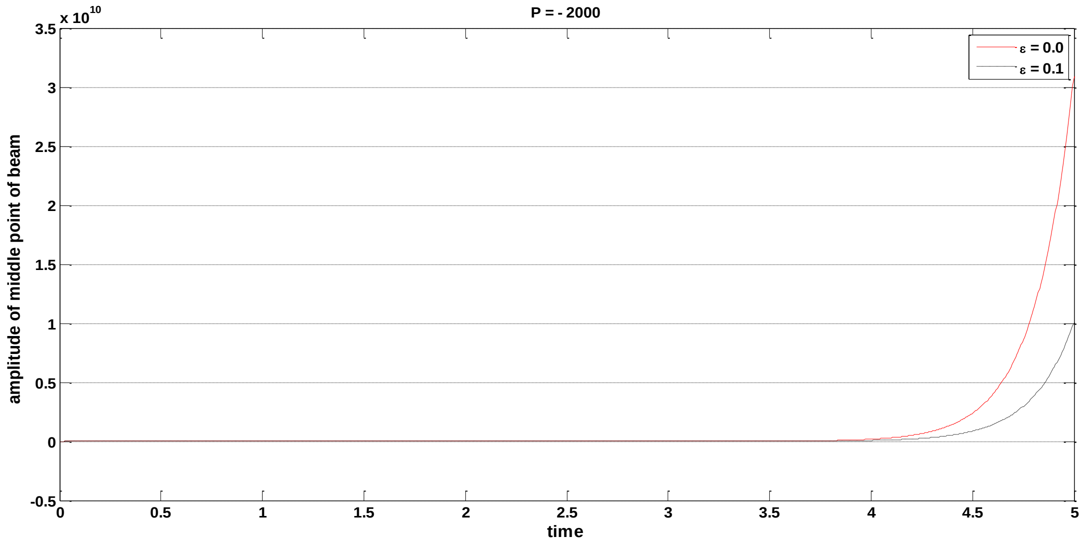

Figure 15. The effect of perturbation parameter (ε) on buckling of a beam.

The effect of the damping constant on the oscillation amplitude of the middle point of the beam for ideal ($\varepsilon = 0$) and non-ideal ($\varepsilon = 0.1$) supports is shown in Figure 16. It could be seen that the oscillation amplitude of the middle point of the beam with nonzero damping constant decreases with time. While, the oscillation amplitude of the beam without damping does not change.

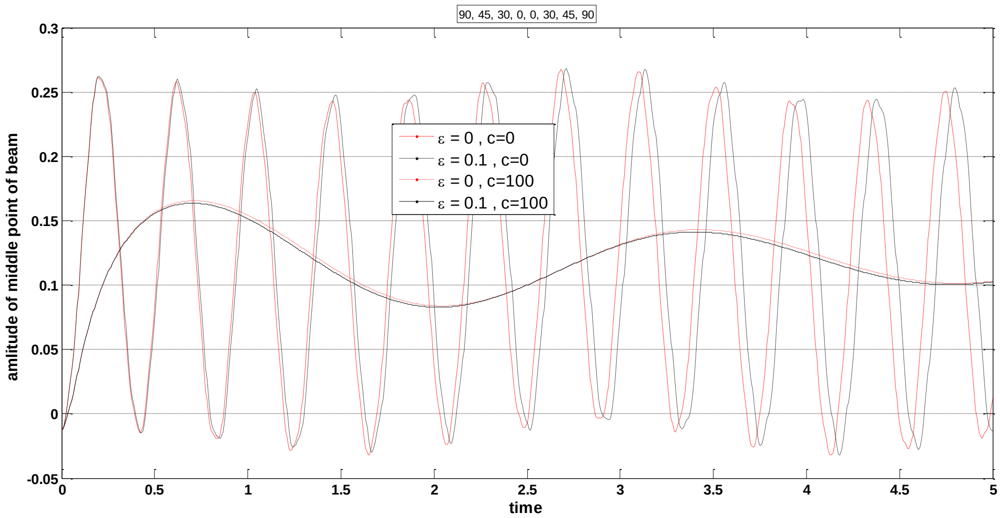

Figure 16. Comparison of vibration of the middle point of beam with ideal and non-ideal support for different damping constant

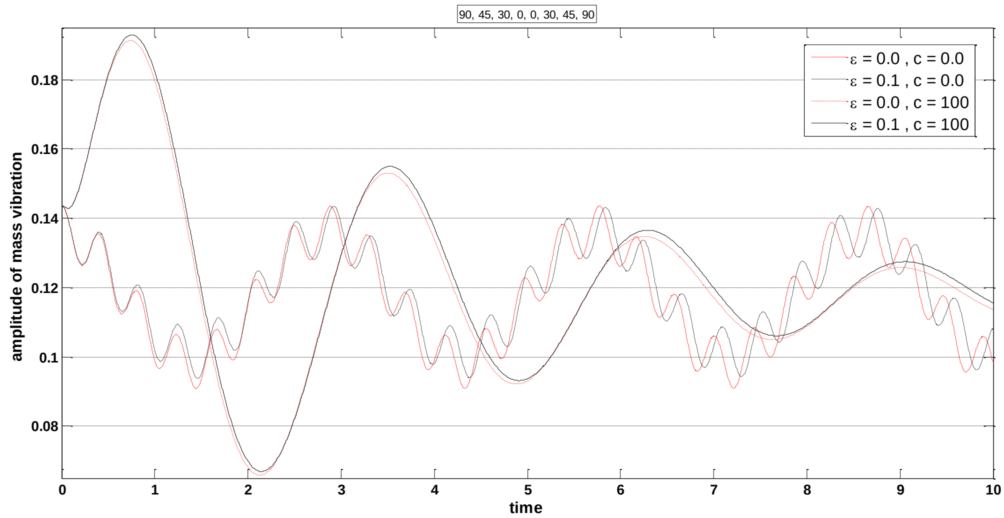

Figure 17. Comparison of vibration of attached mass to the beam with ideal and non-ideal support for different damping constant

The effect of the damping constant on the oscillation amplitude of the attached mass to beam for ideal ($\varepsilon = 0$) and non-ideal ($\varepsilon = 0.1$) supports is shown in Figure 17. It could be seen that the oscillation amplitude of the attached mass to the beam with nonzero damping constant decreases with time. It is shown that at the start of the oscillation, the amplitude of the attached mass to beam without damping is smaller than the amplitude of the attached mass to the beam with damping. The oscillation amplitude of the attached mass to the beam with nonzero damping constant decreases with time.

We know that as the degree of freedom increases, the natural frequency decreases. For example, for a beam with a specified geometry and physical property, natural frequencies based on Euler-Bernoulli beam theory are higher than the natural frequencies based on Timoshenko beam theory. This is because of the degree of freedom which, in Timoshenko beam theory, is more than Euler-Bernoulli beam theory. In the Timoshenko beam theory, the effect of shear deformation, in addition to the effect of rotary inertia, is considered. In the present investigation, according to the obtained results, with increasing perturbation parameter (i.e., ε), the natural frequency decreases and the oscillation amplitude increases. With noting the foregoing expression, this is because of the increasing degree of freedom due to increasing perturbation parameter.

8. Conclusions

The effect of a non-ideal support on free vibrations of an Euler-Bernoulli laminated composite beam carrying an attached mass-spring-damper system under axial force was investigated. The effect of non-ideal support on the oscillation frequency and the amplitude of the beam was studied. The Galerkin method is employed in the displacement field in conjunction with the average acceleration method in the time domain to solve the governing equations of the problem. The results show that the non-ideal boundary conditions may affect the oscillation frequency as well as the amplitude of the beam and the attached mass. The results could be classified as follows:

- The oscillation amplitude and phase difference between the oscillation amplitudes of the composite beam increases as the perturbation parameter (ε) increases. This behavior is independent of the fiber directions of the beam. Increasing the perturbation parameter, the average of the beam oscillation amplitude decreases.
- Increasing the perturbation parameter, the average of the attached mass oscillation amplitude decreases.
- The oscillation amplitude of the beam with ideal supports reduces in some fiber directions. However, the effect of the fiber directions in the oscillation amplitude of the attached mass is only a phase difference.
- When the fiber directions of the beam are symmetric, the fundamental frequency of the beam reaches to its maximum value. Increasing the perturbation parameter results in a decrease in the fundamental frequency of the beam, regardless of the fiber directions of beam.
- The more increase in the tensile axial force results in a less oscillation amplitude of the beam for symmetric fiber directions with ideal supports and vice versa. It means that by increasing the compressive axial force at the same conditions, the oscillation amplitude of the beam increases. The more increase in compressive axial force results in a more increase in the average value of the oscillation amplitude.
- For a specified fiber direction regardless of the kind of axial force, the oscillation amplitude of the beam increases for a semi-ideal supports case ($\varepsilon = 0.1$).
- The oscillation amplitude of the attached mass to the beam is affected from the value and the direction of the axial force and the amount of perturbation parameter.
- Using a non-ideal support postpones the buckling probability of the beam near the first mode of the buckling load. Therefore, the beams having fully-ideal supports would be buckled sooner than the beams with semi-ideal supports.

References

[1] J.W.S. Rayleigh, “The Theory of Sound”. 2rd ed. New York: Dover; 1945.

[2] S. Timoshenko, D.H.Young, W. “Weaver, Vibration Problems in Engineering”. 4rd ed. New York: Wiley; 1974

[3] Ö. Turhan, “On The Fundamental Frequency of Beams Carrying a Point Mass: Rayleigh Approximations Versus Exact Solutions”. Journal of Sound and Vibration, Vol. 230 (2000) No. 2, 449-459.

[4] H. Matsunaga, “Free Vibration and Stability of Thin Elastic Beams Subjected to Axial Forces”. Journal of Sound and Vibration, Vol. 191 (1996) No. 5, 917-933.

[5] J.R. Banerjee, “Free vibration of axially loaded composite Timoshenko beams using the dynamic stiffness matrix method”. Computers and Structures, Vol. 69 (1998) 197-208.

[6] S. Naguleswaran, “Transverse vibration of an uniform Euler–Bernoulli beam under linearly varying axial force”. Journal of Sound and Vibration, Vol. 275 (2004) 47-57.

[7] S. Naguleswaran, “Vibration and stability of an Euler–Bernoulli beam with up to three-step changes in cross-section and in axial force”. International Journal of Mechanical Sciences, Vol. 45 (2003) 1563-1579.

[8] Y. Yesilce, O. Demirdag, “Effect of axial force on free vibration of Timoshenko multi-span beam carrying multiple spring-mass systems”. International Journal of Mechanical Sciences, Vol. 50 (2008) 995-1003.

[9] M. Pakdemirli, H. Boyaci, “Effect of non-ideal boundary conditions on the vibrations of continuous systems”. Journal of Sound and Vibration, Vol. 249 (2002) No. 4, 815-823.

[10] M. Pakdemirli, H. Boyaci, “Non-linear vibrations of a simple–simple beam with a non-ideal support in between”. Journal of Sound and Vibration, Vol. 268 (2003) 331-341.

[11] H. Boyaci, “Beam vibrations with non-ideal boundary conditions”. Springer Proceedings in Physics, Vol. 111 (2007) 97-102.

[12] K. Malekzadeh, S.M.R. Khalili, P. Abbaspour, “Vibration of non-ideal simply supported laminated plate on an elastic foundation subjected to in-plane stresses”. Composite Structures, Vol. 92 (2010) 1478-1484.

[13] S.M.R. Khalili, P. Abbaspour, K. Malekzadeh, “Buckling of non-ideal simply supported laminated plate on Pasternak foundation”. Applied Mathematics and Computation, Vol. 219 (2013) 6420-6430.

[14] L. Jinhee, “Free vibration analysis of beams with non-ideal clamped boundary conditions ”. Journal of Mechanical Science & Technology, Vol. 27 (2013) 297-303.

[15] M. Ghadiri, M. Hosseini, “Vibration Analysis of A Composite Beam with Non-Ideal Boundary Conditions”. International Journal of Basic Sciences & Applied Research, Vol. 3 (2014) 103-118.

[16] S. Rao, Mechanical vibrations. 3rd ed. Wesley: Addison; 1995.

[17] D. Shu, C.N. Della, “Free vibration analysis of composite beams with two non-overlapping delaminations”. International Journal of Mechanical Sciences, Vol. 46 (2004) 509–526.

[18] R.M. Jones, Mechanics of composite materials. 2rd ed. Taylor and Franci: Philadelphia; 1999.

[19] S.A. Siddiqui, M.F. Golnaraghi, G.R. Heppler, “Large free vibration of a beam carrying a moving mass”. International Journal of Non-Linear Mechanics, Vol. 38 (2003) No. 10, 1481-1493.